Civil and Environmental Engineering
Vol. 0, Issue 0, DOI: 10.2478/cee-2026-0109

Post-Fire Performance Enhancement of Pre-loaded RC Short Columns Using CFRP Confinement

Mohanad Wisam MOUSA[1,*], Ahlam Sader MOHAMMED[1], Sarmad Shafeeq ABDULQADER[1]

[1] Civil Engineering Department, University of Technology, Baghdad, Iraq.

* corresponding author: bce.22.56@grad.uotechnology.edu.iq

Date of Submission: 17 February 2026
Revision Date: 17 March 2026
Date of Acceptance: 17 March 2026

Civil and Environmental Engineering
Journal of the Faculty of Civil Engineering | University of Žilina

Abstract

This study presents an experimental investigation on the rehabilitation of fire-damaged reinforced concrete (RC) columns through the removal of the deteriorated concrete cover, its replacement with new normal-strength concrete (NSC), and subsequent full wrapping using carbon fibre-reinforced polymer (CFRP) sheets. The columns were tested under an eccentric load with an eccentricity of e = 90 mm. The experimental program consisted of nine short RC column specimens classified into two groups according to fire exposure temperatures of 500 °C and 700 °C, using a specially designed furnace. In addition, one unexposed control column was tested for comparison. Two fire exposure durations, namely 60 and 120 min, were considered. During fire exposure, the columns were subjected to a pre-applied axial load equal to 50% of the ultimate load capacity of the unexposed control specimen. The experimental results showed that the ultimate load-carrying capacity of the columns decreased with increasing fire temperature and exposure duration. Specifically, columns exposed to 500 °C and 700 °C for 60 and 120 min showed reductions in load-carrying capacity of (11.65%), (14.11%), (20.85%), and (36.8%), respectively, relative to the control column. After rehabilitation using the adopted technique based on NSC replacement and CFRP wrapping, the fire-damaged columns showed improvements in ultimate load-carrying capacity ranging from (32.14%) to (66.02%) relative to the corresponding fire-exposed specimens.

Keywords

CFRP; Fire-damaged RC columns; Fire exposure duration; Eccentric loading; Rehabilitation.

1. Introduction

Columns are among the most critical load-bearing elements in reinforced concrete (RC) structures, as their failure may lead to progressive or total collapse of the structural system. Exposure to fire by accident may significantly reduce the mechanical properties of concrete and steel, resulting in cracks, spalling, reduced stiffness, and a reduction in the capacity to carry axial loads (Mansour Kadhum Alkafaji, 2015). Experimental studies have shown that the residual response of fire-exposed reinforced concrete columns depends on the peak temperature, time of exposure, geometry of the member, quality of concrete, and the presence of sustained axial loads (Ahmed et al., 2019; Kodur et al., 2017; Sarsam et al., 2018).

When the loading is prolonged along with heating, the structural deterioration is hastened, and the post-fire properties, such as strength and stiffness, are substantially reduced (Alhadid & Youssef, 2022). Various analytical and numerical models have been proposed to predict the properties of RC columns after exposure to fire, and reliable

predictions have been made on the properties of RC columns under various fire scenarios (Chen & Jiang, 2022; Jovanović et al., 2023).

Fiber-reinforced polymer (FRP) composites have proven to be a viable option for concrete members that have deteriorated (Yoo & Choo, 2022). The use of external confinement with FRP composites increases the axial strength, ductility, and stiffness of RC columns. CFRP composites have gained significant attention due to their high tensile strength, durability, and resistance to corrosion (Akbulut et al., 2025; Li et al., 2017). Recent studies published in Civil and Environmental Engineering have also confirmed the structural benefits of CFRP-based strengthening in RC columns. (Hasan et al., 2024) reported that different strengthening techniques can improve the load-carrying capacity, stiffness, and ductility of circular RC columns under axial loading, while (Dewi et al., 2024) investigated the tensile-force behaviour and strain response of circular hollow RC columns strengthened with CFRP strips, further demonstrating the contribution of CFRP to enhancing column performance.

Some recent research works have also explored the post-fire rehabilitation of RC columns with the help of CFRP wrapping. The empirical results show the capability of CFRP confinement to restore the axial load-carrying capacity of fire-damaged columns, depending on the extent of damage and the thermal history experienced by the columns (Al-Kamaki et al., 2015; Haris et al., 2024; Noman, Yaqub, et al., 2025). The number of CFRP layers, quality of bonding between FRP and concrete, and section geometry are critical factors influencing strengthening efficiency (Abdel-Hafez et al., 2015; Salameh et al., 2024; Shin et al., 2024). Rectangular columns, in particular, exhibit non-uniform confinement due to stress concentration at corners, while rounding corners improves stress distribution and delays premature rupture of CFRP sheets (Cao et al., 2023; Zhao et al., 2023).

Numerical simulations and advanced predictive models have confirmed the effectiveness of multi-layer CFRP confinement in recovering both strength and ductility of fire-exposed columns (Noman, Salman, et al., 2025; Zhou et al., 2026).

Despite these developments, previous studies have mainly focused on either the post-fire behaviour of RC columns or the effectiveness of CFRP strengthening under relatively simplified conditions. Limited experimental attention has been given to preloaded short RC columns subjected to severe fire exposure and subsequently rehabilitated using a combined repair technique involving damaged concrete cover removal, recasting with new normal-strength concrete NSC, and external confinement with CFRP sheets, particularly under eccentric loading conditions. In addition, the coupled effects of thermal damage, sustained preload, and post-fire rehabilitation on strength recovery, stiffness response, and ductility enhancement have not yet been sufficiently clarified through experimental investigation. Accordingly, the present study aims to fill this gap by experimentally evaluating the behaviour of preloaded fire-damaged RC short columns rehabilitated using the adopted combined rehabilitation strategy, through comparison with corresponding unwrapped fire-damaged columns and unexposed reference specimens.

2. Methodology

2.1. Materials

The materials utilized in this study included concrete, steel reinforcement, and CFRP sheets, as described in the following subsections.

2.1.1. Concrete

All specimens were cast using normal-strength concrete with a measured compressive strength of 32 MPa. The corresponding mix proportions are presented in Table 1.

Table 1: Mix proportions of the concrete used in this study

Materials	Amount
Cement (kg/m^3)	390
Sand (kg/m^3)	685
Gravel (kg/m^3)	1075
w/c (–)	0.47
f′c at 28 days (MPa)	32

2.1.2. Steel

Three types of steel reinforcing bars were utilized in the experimental program. Deformed Ø10 mm bars (Al-Mass production) were used as longitudinal reinforcement for all column specimens. Deformed Ø12 mm bars (Al-Mass production) were employed for reinforcing the corbels, while Ø6 mm deformed bars (Turkish production) served as transverse ties in both the corbels and the column specimens.

2.1.3. Carbon Fiber Reinforced Polymer (CFRP) Sheets

This study used Sika Wrap Hex-230C, a type of CFRP sheets with a width of 50 cm.

3. Specimens Details

All specimens were constructed with identical external dimensions and geometric configurations. The columns consist of a square cross-section with uniform dimensions. Each column has an overall length of 1400 mm and a cross-sectional size of (150 × 150) mm. The clear distance between the two corbels is 800 mm, and each corbel measures (150 × 250 × 300) mm. The corbels were designed to facilitate the application of an eccentric load on the columns. Each column includes a concrete cover of 20 mm and is reinforced with four longitudinal deformed steel bars (ϕ10 mm), resulting in a reinforcement ratio of ρ = 0.0140. Transverse reinforcement consists of 6 mm diameter steel ties spaced at 100 mm. All columns were fabricated in accordance with the requirements of ACI 318-19. Figure 1 presents the detailed reinforcement configurations for both the columns and the corbels. As outlined in Table 2, the experimental program comprises nine normal-strength concrete (NSC) column specimens. One specimen (C_1) serves as the control column and was neither preloaded nor exposed to fire, while the remaining eight specimens were subjected to fire exposure while carrying a preload equal to 50% of the ultimate load (Pu). The experimental work is divided into two groups:

- Group one (C_2–C_5): Columns C_2 and C_3 were exposed to fire at 500 °C for 60 minutes. Afterwards, Column C_3 was subsequently rehabilitated by removing the damaged concrete cover, casting new normal concrete, and applying a CFRP jacket. Columns C_4 and C_5 were exposed to 500 °C for 120 minutes .Column C_5 was rehabilitated using the same procedure as Column C_3.

- Group two (C_6–C_9): The same experimental procedure as Group one was employed for Group two. The only difference was the fire temperature, which was 700 °C.

It is important to point out that all the fire-exposed columns in both groups were subjected to a constant preload of (81.5 kN), corresponding to (50%) of the ultimate load capacity of the unexposed control specimen C_1, which was (163 kN). The eccentric load was applied with a constant eccentricity of (e = 90 mm), corresponding to an eccentricity ratio of (e/h = 0.60), where (h = 150 mm) is the cross-sectional depth of the column. The eccentric load was applied in the same direction for all fire-exposed specimens.

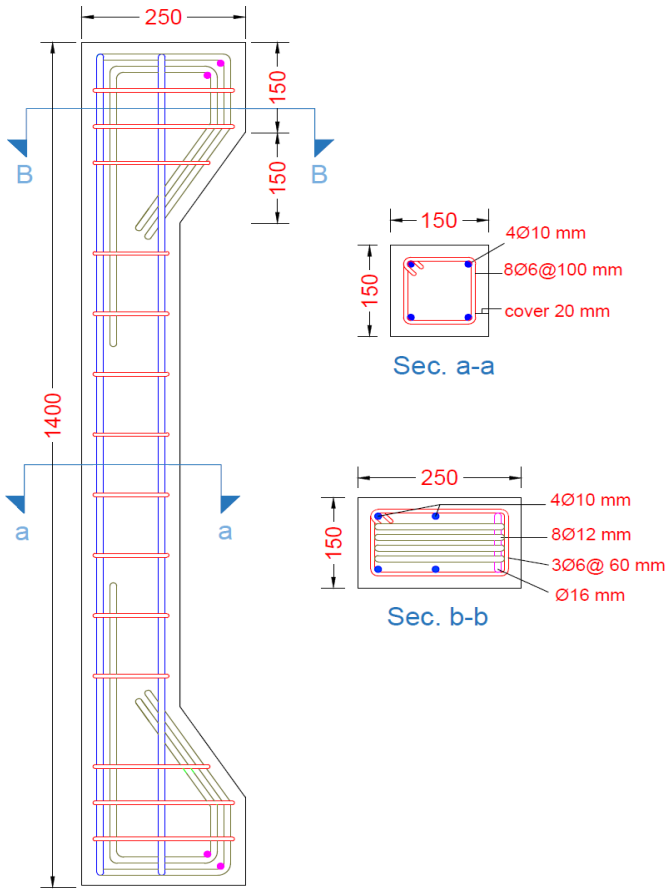

Figure 1: Layout of reinforcement in the tested columns

Table 2: Details of the examined specimens

Group no.	Specimen symbol [Ci]	Fire exposure [Ti] [°C]	Fire duration [Di] [min]	Repair of fire damaged specimen [R]
Control	C_1	-	-	-
One	$C_2\ T_{500}D_{60}$	500	60	-
	$C_3\ T_{500}D_{60}R$	500	60	R
	$C_4\ T_{500}D_{120}$	500	120	-
	$C_5\ T_{500}D_{120}R$	500	120	R
Two	$C_6\ T_{700}D_{60}$	700	60	-
	$C_7\ T_{700}D_{60}R$	700	60	R
	$C_8\ T_{700}D_{120}$	700	120	-
	$C_9\ T_{700}D_{120}R$	700	120	R

4. Casting Procedures

A central batching mixer with a capacity of 10 m^3, supplied by Al-Mustaqbal Ready-Mix Concrete Company, was used to produce the concrete for this study. Before casting, the internal surfaces of the cube and cylinder molds were thoroughly cleaned and lubricated to prevent bonding with the hardened concrete. Each steel reinforcement cage for the column was positioned horizontally in the timber formwork and securely fixed. Concrete was cast in a single layer in each mold, and compaction was done by hand before two minutes of vibration using an internal vibrator. Normal practices for

placing each layer and rodding were strictly adhered to for proper compaction of the concrete in the molds for the cube and cylinder, as shown in Figure 2.

5. Fire Test

The columns were subjected to the fire exposure test after a few months, using a brick furnace with dimensions 1400 × 1400 × 1150 mm, as shown in Figure 3. Two different exposure times were used: 60 and 120 minutes, with the furnace temperatures set to 500 °C and 700 °C, respectively. The furnace temperatures were regulated automatically by a digital system and a gas regulator, as shown in Figure 3. The temperatures were measured using K-type thermocouples with a diameter of 4 mm. The cover of the furnace was removed after the completion of the heating to simulate the natural cooling process. Accordingly, only gradual air cooling was considered in the present study to ensure a controlled and consistent post-fire condition for all fire-exposed specimens. The region of the column subjected to the fire exposure test was 800 mm in length. The columns were subjected to eccentric loading. Column C_1 was used as the control specimen and was not subjected to the fire exposure test, whereas columns C_2 to C_9 were preloaded to 81.5 kN, equivalent to 50% of the ultimate axial load capacity, as shown in Figure 4. The preload level was determined based on 50% of the ultimate load capacity of the unexposed control specimen (C_1), and it was selected to simulate a sustained service-level loading condition. The preload was applied before heating and maintained throughout both the fire exposure and the subsequent cooling stage. A detailed description of the furnace, the testing setup, and the preloading system are provided in Figure 4. The average furnace temperature recorded during the fire tests was compared with the ASTM E119-20 time-temperature curve, as shown in Figure 5. Temperature monitoring in the present study was based on thermocouples installed inside the furnace only.

Figure 2: Casting process phases

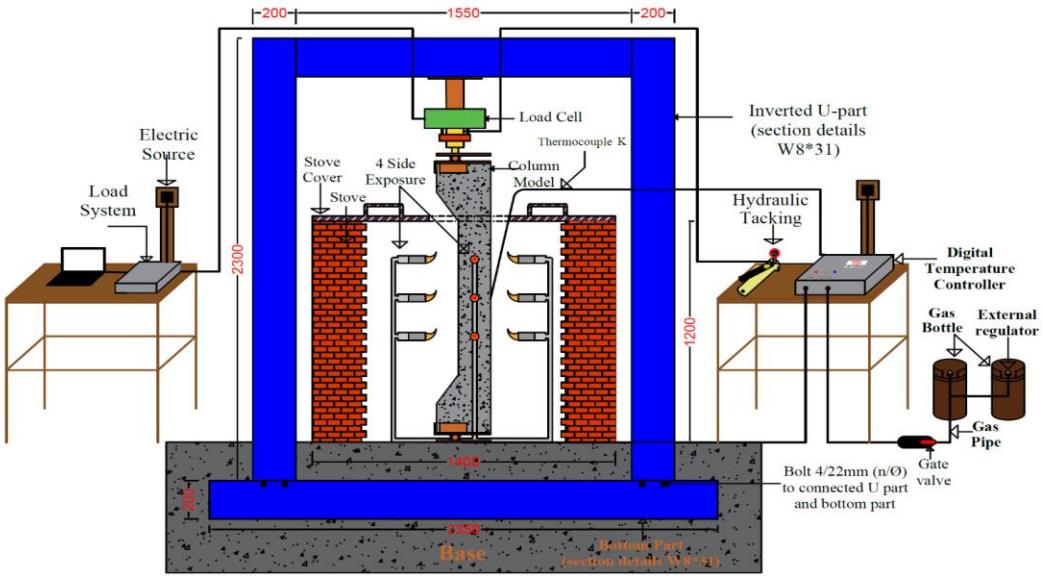

Figure 3: Description of the loading frame

Figure 4: Specimens subjected to fire exposure under pre-loading curve

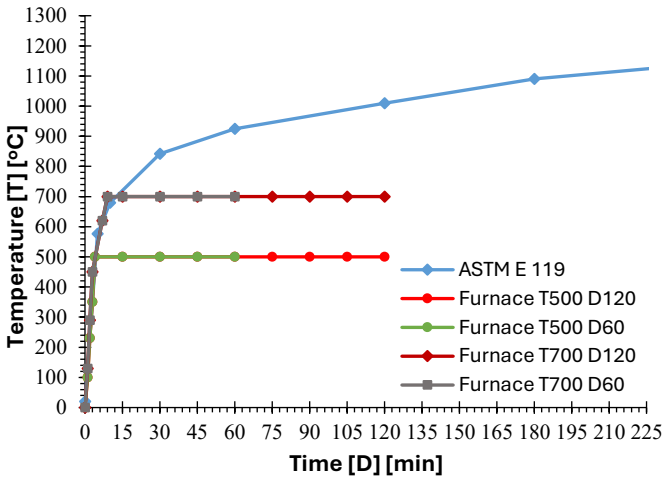

Figure 5: Measured average furnace temperature versus ASTM E119-20 time-temperature curve

6. Repair of Fire-Damaged Column Specimens

The rehabilitation of fire-exposed columns (C_3, C_5, C_7, and C_9) involved the following key procedures: The adopted rehabilitation strategy involved a combined repair technique including removal of the damaged concrete cover, recasting with new normal-strength concrete NSC, and external confinement using CFRP sheets. Accordingly, the post-repair structural response reflects the combined effect of the adopted rehabilitation measures.

a. Removal of Damaged Concrete: The damaged exterior concrete layer was carefully removed manually until all longitudinal reinforcement was exposed. Mechanical methods were avoided to prevent any dynamic vibration that may affect the integrity of the column structures. The adopted removal procedure was intentionally limited to the visibly damaged exterior concrete cover in order to simulate a practical rehabilitation technique for fire-damaged columns, rather than complete removal of all concrete that may have been thermally affected by fire exposure.

b. Installation of Shear Connectors: 4 mm-diameter shear connectors were horizontally installed on all sides of the stirrups to ensure a reliable bond between the original concrete core and the new layer of Normal Concrete (NC).

c. Epoxy Preparation and Application: The epoxy resin (Sikadur®-32 LP) was prepared by separately stirring the base and hardener, followed by thorough mixing with a slow-speed drill for two minutes until a uniform colour was achieved. Approximately 90 minutes prior to casting the NC layer, the cleaned surface of the existing concrete was coated with epoxy to enhance adhesion between the old and new concrete layers.

d. The new layer of Normal strength Concrete (NSC) with a compressive strength of 29.4 MPa was cast and subjected to curing for 28 days. All processes are represented in Figure 6.

e. For the application of CFRP sheets on the fire-exposed columns, the following steps were carried out:

1. CFRP Sheet Preparation: The CFRP sheets were cut to the required dimensions, and the concrete was meticulously cleaned to ensure the absence of impurities.

2. Epoxy Preparation: The two parts of the epoxy adhesive material (Sikadur-330, A and B) were mixed in a ratio of 4:1, respectively, until a uniform colour was achieved.

3. Epoxy Application: The epoxy coating with a thickness of about 1.5 mm was applied to the column surface and the CFRP sheets.

4. CFRP Sheet Installation. The CFRP sheets were accurately placed in their respective positions on the column surface previously coated with epoxy. A rubber roller was used to press the sheets to ensure complete adhesion to the column surface and to remove excess epoxy from both sides of the sheets. Excess epoxy was then removed from the edges of the CFRP sheets, as shown in Figure 6.

5. CFRP Sheet Installation. The CFRP sheets were accurately placed in their respective positions on the column surface previously coated with epoxy. A rubber roller was used to press the sheets to ensure complete adhesion to the column surface and to remove excess epoxy from both sides of the sheets. Excess epoxy was then removed from the edges of the CFRP sheets, as shown in Figure 6.

It should be noted that each test condition was represented by one specimen only in the present experimental program. Therefore, the results are discussed within the scope of the tested specimens, and statistical variability was not evaluated.

Figure 6: Sequential steps of RC column repair

7. Test Setup and Procedure

The specimens were subjected to monotonic loading by a universal testing machine with a maximum capacity of 2500 kN. The load cell was placed at the base of the machine and was connected to a data logger to continuously monitor the applied load. The specimens were subjected to a continuous increase in load until failure. The response of the specimens to the applied load was recorded. Two Linear Variable Differential Transformers (LVDTs) were placed along the height of the eccentric columns to monitor the axial and lateral deflections. In particular, two LVDTs were placed at the base of the columns to monitor the axial deflections of the columns at the various stages of loading, while one LVDT was placed at the mid-height of the columns to monitor the lateral deflections. The measurements were taken at various stages of loading until the specimens failed. The required safety precautions were taken to monitor the cracks developing in the specimens. A detailed evaluation of the failure modes, crack patterns, and ultimate capacity of the columns was carried out, as presented in Figure 7.

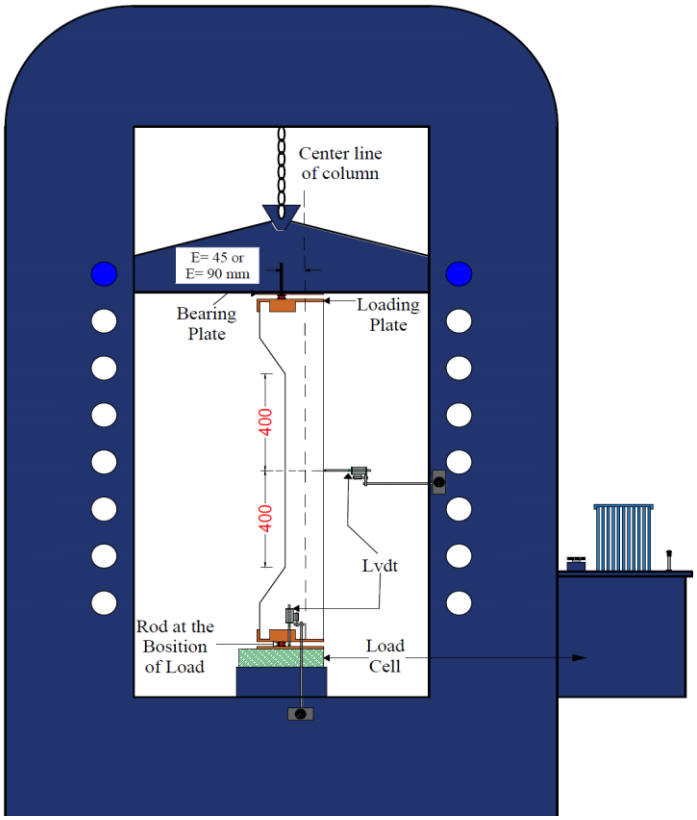

Figure 7: Test setup with instrumentation details

8. Results and Discussion

The experimental results for the columns were compared systematically with the results of the other specimens to assess the effect of the duration of exposure to fire and the intensity of the temperature, under constant pre-load and eccentricity of the load. The parameters studied were the failure mode, ultimate load capacity, initial cracking load, and the axial deformations of the columns. A summary of the findings is presented in Table 3.

Table 3: Results of laboratory testing on column specimens

Group no.	Specimen symbol [Ci]	Ultimate load capacity [kN]	Reduction in ultimate load relative to control [%]	Enhancement in ultimate load relative to control [%]	Recovery in ultimate load relative to corresponding fire-damaged specimen [%]	Ultimate axial deformation [mm]	Ultimate mid-height lateral deflection [mm]
Control	C_1	163	0	0	-	9.3	13.85
One	$C_2\ T_{500}D_{60}$	144	11.65	-	-	8.27	14.67
	$C_3\ T_{500}D_{60}R$	197	-	20.86	36.81	11.9	15.24
	$C_4\ T_{500}D_{120}$	140	14.11	-	-	8.67	15.14
	$C_5\ T_{500}D_{120}R$	185	-	13.5	32.14	11.05	17.2
Two	$C_6\ T_{700}D_{60}$	129	20.85	-	-	10.34	16.42
	$C_7\ T_{700}D_{60}R$	174	-	6.75	34.88	10.84	17.27
	$C_8\ T_{700}D_{120}$	103	36.8	-	-	11.42	18.21
	$C_9\ T_{700}D_{120}R$	171	-	4.91	66.02	13.83	19.41

8.1. Load Carrying Capacity

The load-carrying capacity refers to the ultimate maximum load that the specimens of the columns can withstand before any discernible reduction in the readings of the testing equipment is observed, accompanied by rapid deformation that signifies failure. The results show that the fire-exposed columns in the first group had a better residual load-carrying capacity compared to those in the second group, which is consistent with expectations due to the lower level of exposure.

Relative to the unexposed reference column, the ultimate load carrying capacity of specimens $C_2T_{500}D_{60}$ and $C_4T_{500}D_{120}$ in the first group, which were exposed to a temperature of 500 °C for durations of 60 and 120 minutes, respectively, decreased by (11.65% and 14.11%). Subsequently, the fire-damaged columns $C_3T_{500}D_{60}R$ and $C_5T_{500}D_{120}R$ were rehabilitated by removing the deteriorated concrete cover and replacing it with normal-strength concrete (NSC), followed by full wrapping of the columns using carbon fibre reinforced polymer (CFRP). The results demonstrated that the adopted rehabilitation technique effectively restored and enhanced the ultimate load capacity, achieving increases of (20.86% and 13.5%), respectively, relative to the reference column.

When the exposure temperature was increased to 700 °C for 60 and 120 minutes, the second group specimens $C_6T_{700}D_{60}$ and $C_8T_{700}D_{120}$ exhibited more pronounced reductions in ultimate load-carrying capacity of (20.85% and 36.8%), respectively, relative to the reference column. After rehabilitation using NSC with CFRP sheets, columns $C_7T_{700}D_{60}R$ and $C_9T_{700}D_{120}R$ showed noticeable improvements in load-carrying capacity following rehabilitation, with increases of (6.75% and 4.91%), respectively, relative to the reference column, as also reported by (Cao et al., 2023). As illustrated in Figure 8.

Relative to the corresponding fire-damaged columns, the adopted rehabilitation technique based on NSC with CFRP sheets significantly improved the load-carrying capacity of the rehabilitated reinforced concrete columns. For the specimens exposed to 500 °C, columns $C_3T_{500}D_{60}R$ and $C_5T_{500}D_{120}R$ exhibited increases in ultimate load capacity of (36.81%) and (32.14%), respectively, compared with their corresponding fire-damaged columns $C_2T_{500}D_{60}$ and $C_4T_{500}D_{120}$. For the specimens exposed to 700 °C, columns $C_7T_{700}D_{60}R$ and $C_9T_{700}D_{120}R$ showed improvement ratios of (34.88%) and (66.02%), respectively, compared with their corresponding fire-damaged columns $C_6T_{700}D_{60}$ and $C_8T_{700}D_{120}$.

8.2. Load-Displacements Relationship

A clear convergence was observed between the lateral and axial displacement responses, both reflecting an increase in ultimate displacement with rising fire exposure temperature. The adopted rehabilitation technique based on NSC with CFRP sheets led to an improvement in the displacement response of the columns under loading. Selected load-displacement curves are illustrated in Figures (9-14). The load-deflection responses of the second group demonstrated greater sensitivity to elevated temperatures than those of the first group. Nevertheless, this rehabilitation technique did not produce any noticeable improvement in the displacement performance of the second-group specimens.

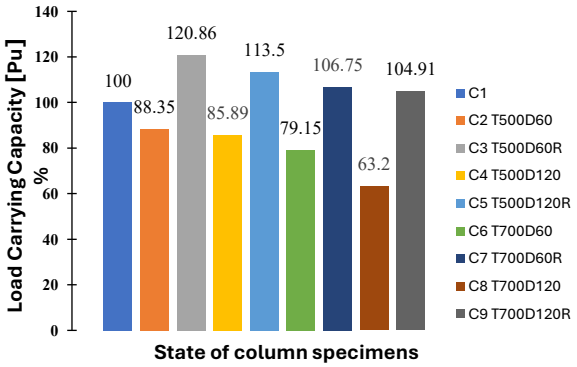

Figure 8: Percentage of load carrying capacity for the tested column specimens

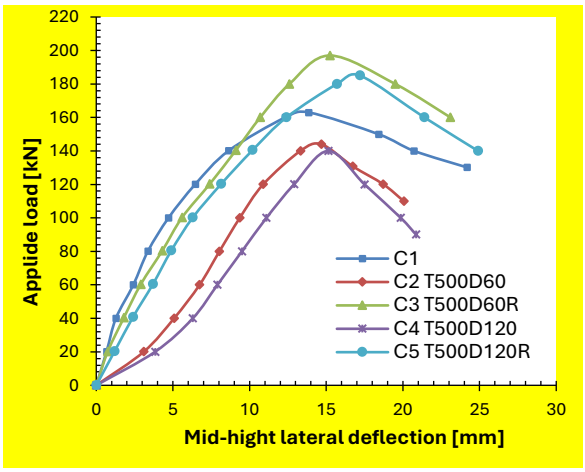

Figure 9: Load-deflection curves of group one columns

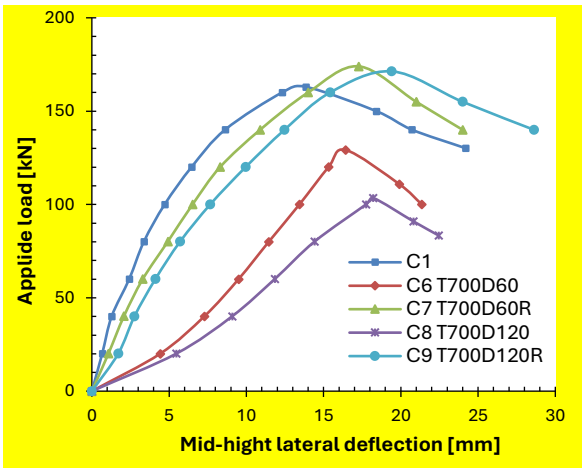

Figure 10: Load-deflection curves of group two columns

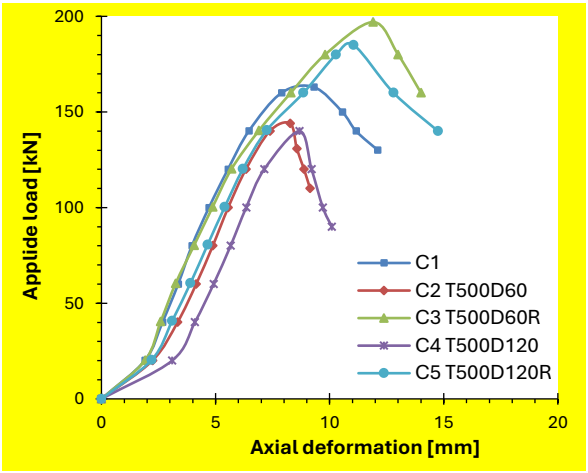

Figure 11: Load – axial deformation of group one columns

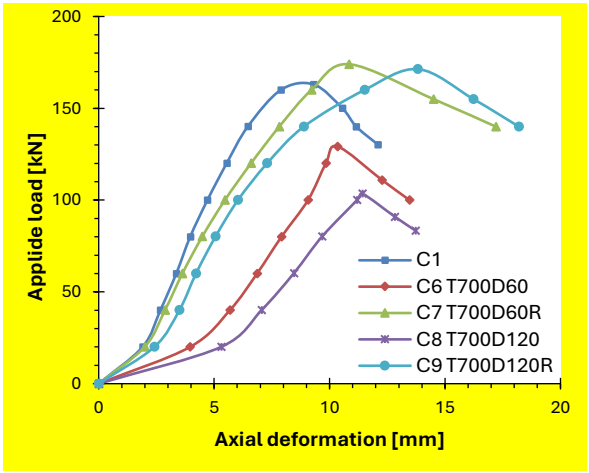

Figure 12: Load – axial deformation of group two columns

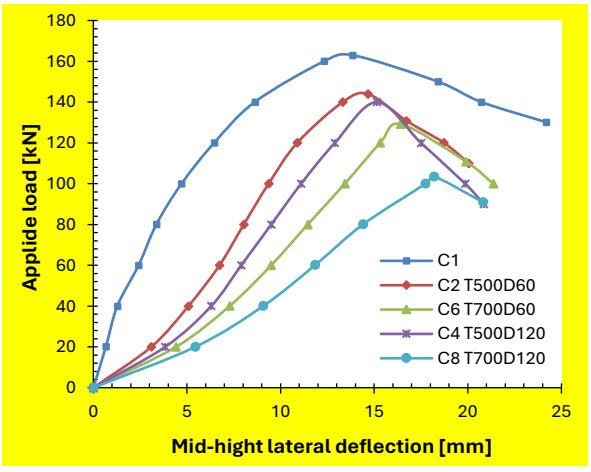

Figure 13: Load –deflection of exposed to 500°C and 700°C

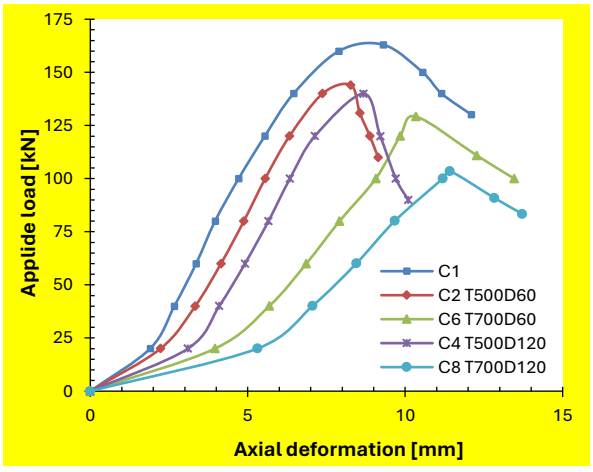

Figure 14: Load – axial deformation of exposed to 500°C and 700°C

8.3. First Crack Load

Crack widths were measured using a crack gauge, while the initiation of the first visible crack was identified through direct visual observation and the corresponding load was recorded. In eccentrically loaded column specimens, transverse flexural cracks typically initiate in the tension zone and propagate toward the compression zone. The black-coloured cracks were associated with the effects of eccentric loading during mechanical testing, whereas the red-coloured cracks were attributed to axial loading effects following fire exposure. Based on Table 4, the non-fire-exposed reference columns exhibited the smallest crack widths among all specimens, with an average value of (0.4 mm) , as illustrated in Figure 15a. In contrast, the fire-exposed columns showed larger average crack widths ranging from (0.44 to 0.69)mm after fire exposure and subsequent mechanical testing, as presented in Figure 15b. This increase is primarily attributed to the detrimental effects of elevated temperatures on the concrete microstructure. No visible external cracks were observed on the rehabilitated columns after repair, since their surfaces were fully wrapped with CFRP sheets. Therefore, direct observation of surface crack development was visually restricted by the external confinement layer.

Table 4: Crack width and observed crack location of the tested columns

Group no.	Specimen symbol [Ci]	Maximum visible crack width after fire exposure before repair [mm]	Visible crack width at service load during mechanical testing [mm]	Location of crack
Control	C_1	-	0.4	In the last quarter of the column
One	C_2 $T_{500}D_{60}$	0.16	0.62	In the middle of the column
	C_3 $T_{500}D_{60}R$	0.18	Not visible due to CFRP wrapping	Not visually observable after rehabilitation
	C_4 $T_{500}D_{120}$	0.4	0.66	In the last quarter of the column
	C_5 $T_{500}D_{120}R$	0.32	Not visible due to CFRP wrapping	Not visually observable after rehabilitation
Two	C_6 $T_{700}D_{60}$	0.48	0.68	In the first quarter of the column
	C_7 $T_{700}D_{60}R$	0.56	Not visible due to CFRP wrapping	Not visually observable after rehabilitation
	C_8 $T_{700}D_{120}$	0.74	0.8	In the middle of the column
	C_9 $T_{700}D_{120}R$	0.9	Not visible due to CFRP wrapping	Not visually observable after rehabilitation

8.4. Failure Mode

In general, all the column specimens were subjected to a constant eccentricity of e = 90 mm. The columns exposed to this type of loading condition have mainly exhibited compression-controlled failure. The failure mechanism was progressive in nature, starting from the tension face of the column and then progressing toward the compression face. In the unexposed reference column, crack initiation and growth were relatively slow and limited in extent when compared with the fire-exposed specimens. Conversely, columns subjected to fire exposure contained pre-existing microcracks induced by thermal degradation, which significantly accelerated crack initiation, propagation, and widening at relatively lower load levels, as illustrated in Figures 16 (a to i). An extended period of fire exposure enabled the development of cracks. Concrete specimens exposed to fire for 120 minutes showed wider and more extensive cracks compared to specimens exposed to fire for 60 minutes under the same temperature condition. Failure always resulted in spalling of the concrete cover in the compression zone in the middle third of the column. Subsequent crushing of the concrete cover started from the middle height and progressed to longitudinal and transverse cracking before finally detaching from the column, as depicted in Figures 15 and 16 (a to i).

For the rehabilitated columns repaired using NSC with external CFRP sheets, failure was characterized by rupture of the CFRP sheets on the tension side and spalling of the concrete on the compression side, accompanied by noticeable

column buckling, as shown in Figure 16. The failure mode of the fire-damaged rehabilitated columns was generally similar to that of the corresponding unrepaired fire-damaged columns, although the adopted rehabilitation technique improved the overall load resistance and delayed the progression of surface damage. The externally applied CFRP sheets provided lateral confinement, which enhanced the resistance of the rehabilitated columns to concrete spalling under the applied load. Accordingly, the load-resisting mechanism in the rehabilitated columns reflected the combined action of the repaired concrete section and the external CFRP confinement. Although the direct contribution of the CFRP sheets to axial compression resistance was limited because of their relatively small thickness and fibre orientation, their confinement effect played an important role in improving the behaviour of the rehabilitated columns. The primary function of the CFRP sheets was to provide hoop confinement, thereby restraining lateral expansion of the concrete core, reducing premature spalling, and promoting a more stable post-cracking response. Under axial loading, the rehabilitated column relied on the CFRP layer primarily to resist hoop tensile stresses, while the confined concrete core remained under triaxial compression (Khalaf et al., 2025). Therefore, the CFRP sheets contributed indirectly but effectively to enhancing the load-carrying capacity and ductility of the rehabilitated columns through confinement rather than direct axial load resistance.

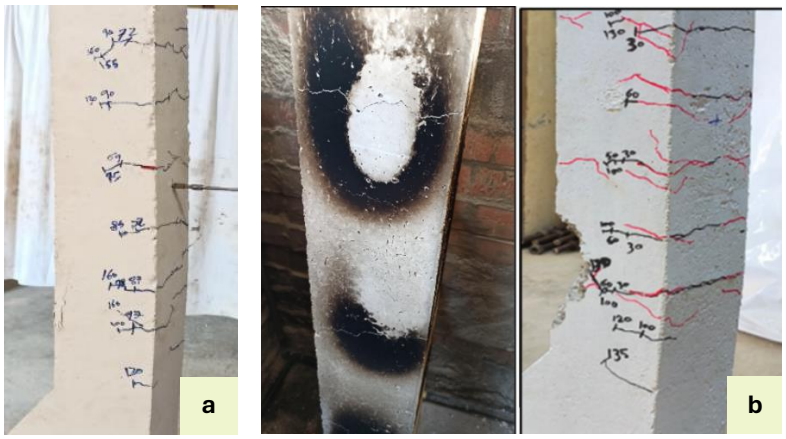

Figure 15: Spread of crack in specimens, **a.** Column specimens without fire, **b.** Column specimens with fire exposure

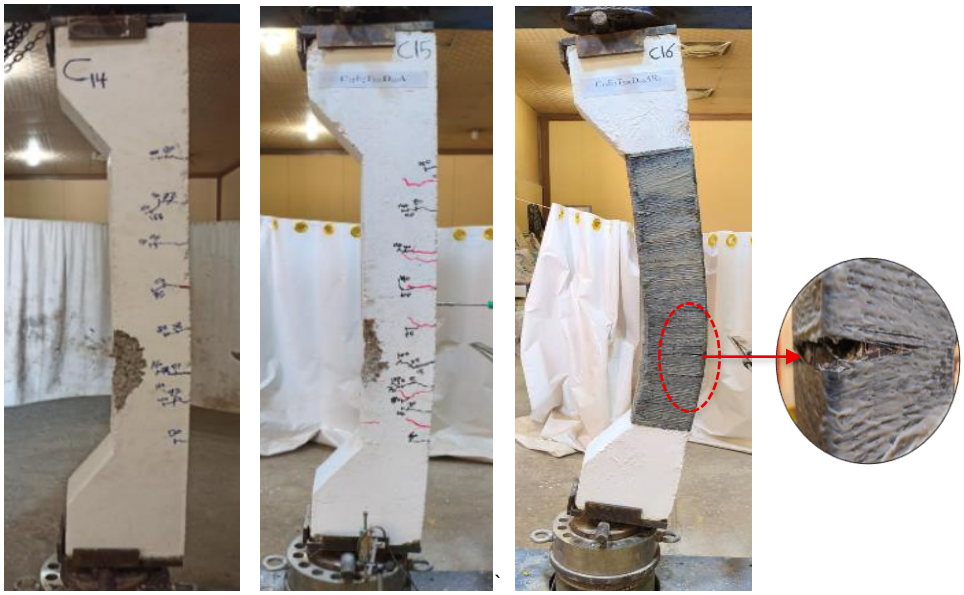

a. C_1 **b.** C_2 $T_{500}D_{60}$ **c.** C_3 $T_{500}D_{60}R$

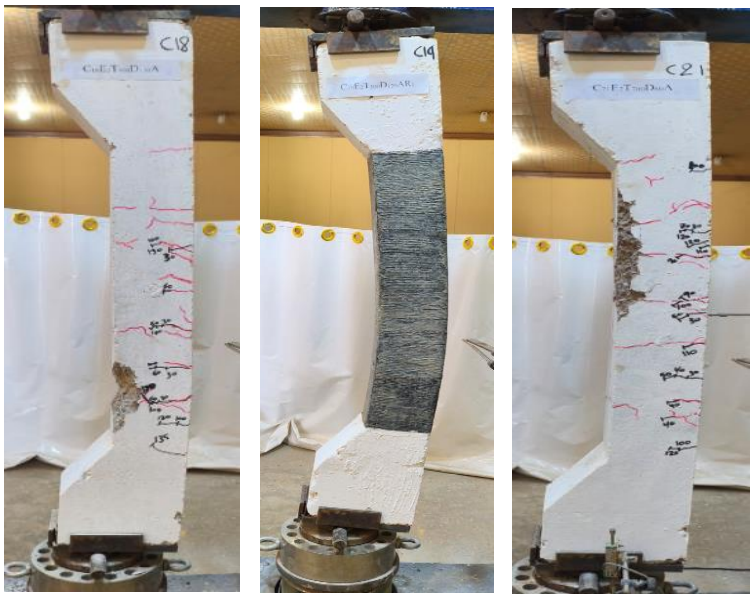

d. $C_4\ T_{500}D_{120}$ **e.** $C_5\ T_{500}D_{120}R$ **f.** $C_6\ T_{700}D_{60}$

Figure 16: Failure modes of columns after testing

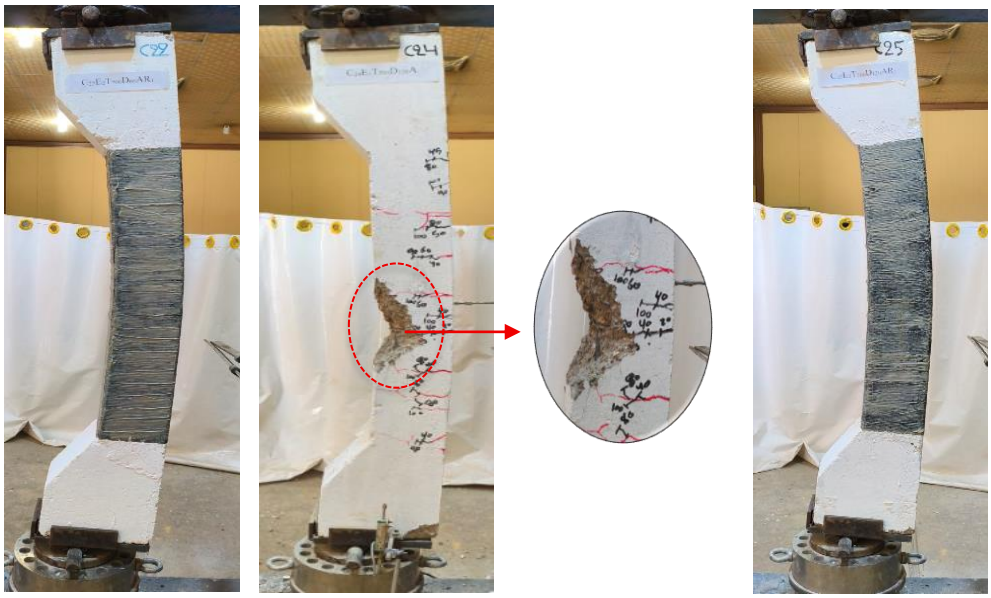

g. $C_7T_{700}D_{60}R$ **h.** $C_8\ T_{700}D_{120}$ **i.** $C_9\ T_{700}D_{120}R$

Figure 16: Failure modes of columns after testing

8.5. Ductility

In this study, the energy absorption capacity approach was adopted to evaluate the ductility of reinforced concrete columns. The energy absorption capacity of a concrete column is defined as the area under the load-displacement curve based on the lateral displacement response up to the failure point. The ductility values were determined numerically by calculating the area under the load-lateral displacement curve for each specimen up to its corresponding failure point. The calculated areas beneath these curves, which represent the ductility of the columns, are presented in Figure 17.

The results show that the ductility of fire-damaged columns improved significantly after applying the adopted rehabilitation technique based on NSC with CFRP sheets. The improvement in ductility was found to be (103.05%) for the columns exposed to 500 °C, whereas for the columns exposed to 700 °C, the improvement was (120.4%). The results obtained in the present study demonstrate the effectiveness of the adopted rehabilitation technique in enhancing the ductility of reinforced concrete columns. The results obtained are in agreement with the conclusions drawn by (Gao et al., 2025), who indicated that confinement of concrete using FRP sheets can significantly enhance its strength, ductility, and energy absorption capacity.

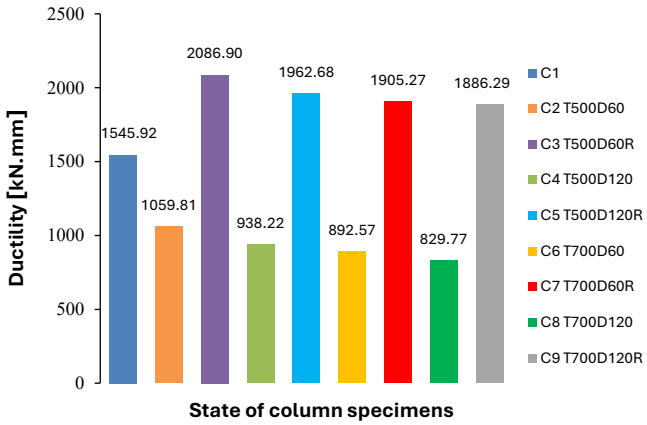

Figure 17: Ductility of specimens

8.6. Stiffness Parameter

In the context of structural mechanics, the definition of stiffness is given by the magnitude of the load required to cause unit deformation in the structural member. The commonly used technique to measure the stiffness is the secant slope technique, where the stiffness is determined by the slope of the curve at 75% of the ultimate load, as proposed by (Lan et al., 2025; Muthuswamy & Thirugnanam, 2014). In the present study, this parameter was adopted as a consistent comparative stiffness index for all tested specimens. As illustrated in Figure 18, the stiffness of the columns is determined, followed by the comparison with the reference specimen. From the results, it is evident that the stiffness is reduced with the increase in fire exposure temperature and duration. The reduction is significant at 700 °C, where the stiffness is reduced by 70.03%, along with the reduction in the load-carrying capacity.

On the other hand, when the adopted rehabilitation technique based on damaged concrete cover replacement with NSC and external confinement using CFRP sheets was applied, no significant improvement in stiffness was observed. In fact, a reduction in stiffness was recorded by (21.06%) for columns exposed to 500 °C after rehabilitation and by (31.45%) for those exposed to 700 °C. This limited stiffness response may be attributed not only to the characteristics of the CFRP sheets, which mainly enhance confinement and tensile resistance rather than the initial axial stiffness of the section, but also to the influence of pre-existing fire-induced damage, the properties of the recast NSC layer, and the interaction between the original concrete core and the repaired outer layer. As mentioned in the literature, CFRP has high tensile strength but negligible compressive strength, especially when used in thin sheets. Accordingly, the initial stiffness of the rehabilitated columns remained governed mainly by the concrete core and internal steel reinforcement, while the confinement effect of CFRP sheets became more relevant after the development of lateral dilation. Thus, the adopted rehabilitation technique showed negligible effectiveness in improving the initial stiffness of fire-damaged RC columns.

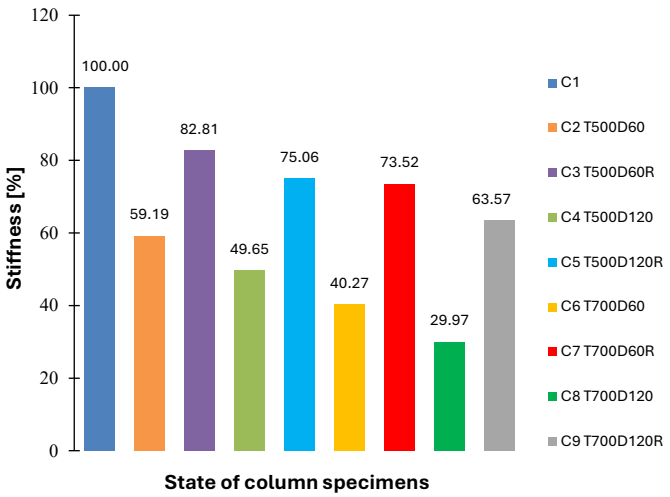

Figure 18: Stiffness of specimens

9. Conclusions

Based on the experimental findings, the following conclusions can be drawn regarding the behaviour of the investigated columns:

1) After fire exposure, the specimens exposed to 500 °C exhibited higher stiffness than those exposed to 700 °C. This is attributed to the more severe thermal damage caused by the higher temperature, which adversely affected the concrete and reinforcing steel.

2) Increasing the fire exposure duration led to a reduction in the load-carrying capacity of the columns. The ultimate load capacity decreased by (11.65%) and (14.11%) after exposure to 500 °C for 60 and 120 min, respectively, compared with the reference column. More pronounced reductions of (20.85%) and (36.80%) were observed after exposure to 700 °C for the same durations.

3) The crack pattern observations indicated that increasing fire temperature and exposure duration had a marked effect on the cracking behaviour of the preloaded fire-exposed columns.

4) The specimens repaired using the adopted rehabilitation technique, in which the damaged concrete cover was removed, replaced with new NSC, and externally confined with CFRP sheets, showed recovery in load-carrying capacity.

5) The experimental results showed that the adopted rehabilitation technique improved the load-carrying capacity of the fire-damaged columns by (32.14% to 66.02%) compared with the corresponding fire-exposed specimens, and enhanced ductility by (103.05% to 120.4%) compared with the burned columns. However, the same rehabilitation technique showed limited effectiveness in improving stiffness.

6) It should be noted that the conclusions drawn in this study are limited to specimens subjected to gradual air cooling after fire exposure. Different cooling regimes, particularly rapid cooling resulting from firefighting water, may lead to different residual structural behaviour and post-fire performance.

Author Contributions

M.M. conducted the experiments, conceptualized the study, developed the methodology, performed the investigation, validation, visualization, and data analysis, and wrote the original draft. **A.M.** contributed to the experimental work, supervised the study, developed the methodology, and reviewed and edited the manuscript. **S.A.** contributed to the experimental work, supervised the research process, reviewed and edited the manuscript, and provided technical support during the study**.**

Disclosure of Interest

The authors declare no conflict of interest, financial or otherwise.

Data Availability Statement

The data sets used and/or analysed during this study are available from the corresponding author [**M.M.**] upon request.

References

Abdel-Hafez, L. M., Abouelezz, A. E. Y., & Hassan, A. M. (2015). Behavior of RC columns retrofitted with CFRP exposed to fire under axial load. HBRC Journal, 11(1), 68–81. https://doi.org/https://doi.org/10.1016/j.hbrcj.2014.02.002.

Ahmed, A., Hasan, S., & Khalaf, A. (2019). Study the Behavior of High Performance Concrete Circular Short Columns Confined by CFRP. Engineering and Technology Journal, 37(7A), 273–281. https://doi.org/10.30684/etj.37.7A.8.

Akbulut, Y. E., Nayır, S., Altunışık, A. C., Kahya, V., Sünnetci, M. O., & Ersoy, H. (2025). Effectiveness of FRP wrapping of heat-damaged concrete in compression for different cooling procedures. Materials and Structures, 58(4), 156. https://doi.org/10.1617/s11527-025-02683-0.

Al-Kamaki, Y. S. S., Al-Mahaidi, R., & Bennetts, I. (2015). Experimental and numerical study of the behaviour of heat-damaged RC circular columns confined with CFRP fabric. Composite Structures, 133, 679–690. https://doi.org/https://doi.org/10.1016/j.compstruct.2015.07.116.

Alhadid, M. M. A., & Youssef, M. A. (2022). Residual Axial Behavior of Restrained Reinforced Concrete Columns Damaged by a Standard Fire. In Fire (Vol. 5, Issue 2). https://doi.org/10.3390/fire5020042.

Cao, V. Van, Dinh, L. H., Trinh, L. C., & Vo, H. B. (2023). Behavior of postfire RC columns retrofitted with CFRP wraps under monotonic and cyclic axial loadings: Experiments and theoretical analyses. Journal of Building Engineering, 72, 106657. https://doi.org/10.1016/j.jobe.2023.106657.

Chen, Q., & Jiang, Y. (2022). Performance Evaluation of Reinforced Concrete Columns under Simultaneously Combined Fire and Cyclic Loads. Buildings, 12(7), 1062. https://doi.org/10.3390/buildings12071062.

Dewi, S. H., Thamrin, R., Haris, S., & Yastari, F. P. (2024). Tensile Forces Behavior on Longitudinal Reinforcement and CFRP Strips on Circular Hollow Reinforced Concrete Columns. Civil and Environmental Engineering, 20(1), 86–97. https://doi.org/10.2478/cee-2024-0008.

Gao, W.-Y., Liang, J., Wang, T.-C., & Ouyang, L.-J. (2025). Postfire Axial Compression Behavior of Unloaded RC Columns Strengthened with CFRP Jackets. Journal of Composites for Construction, 29(6). https://doi.org/10.1061/JCCOF2.CCENG-5189.

Haris, M., Xiong, E., Gao, W., Samuel, M. A., Sahar, N. U., & Saleem, A. (2024). Strengthening Reinforced Concrete Members Using FRP—Evaluating Fire Performance, Challenges, and Future Research Directions: A State-of-the-Art Review. Polymers, 17(1), 13. https://doi.org/10.3390/polym17010013.

Hasan, A. T., Mashrei, M. A., & Makki, J. S. (2024). Behavior of Circular Reinforced Concrete Columns Strengthened by Different Techniques Subjected to Axial Loading. Civil and Environmental Engineering, 20(1), 319–331. https://doi.org/10.2478/cee-2024-0025.

Jovanović, B., Caspeele, R., Lombaert, G., Reynders, E., & Van Coile, R. (2023). State-of-the-art review on the post-fire assessment of concrete structures. Structural Concrete, 24(4), 5370–5387. https://doi.org/10.1002/suco.202201108.

Khalaf, S., Abed, F., El Refai, A., Alhoubi, Y., Ramzi, S., & Hajiloo, H. (2025). PBO-FRCM and CFRP strengthened reinforced concrete columns: In fire and post-fire behavior. Construction and Building Materials, 489, 142306. https://doi.org/10.1016/j.conbuildmat.2025.142306.

Kodur, V., Hibner, D., & Agrawal, A. (2017). Residual response of reinforced concrete columns exposed to design fires. Procedia Engineering, 210, 574–581. https://doi.org/10.1016/j.proeng.2017.11.116.

Lan, S., Liu, Y., Mao, D., & Wang, D. (2025). Experimental and theoretical study on flexural rigidity reduction of reinforced concrete eccentric column. Scientific Reports, 15(1), 29268. https://doi.org/10.1038/s41598-025-15363-4.

Li, X., Lu, J., Ding, D.-D., & Wang, W. (2017). Axial strength of FRP-confined rectangular RC columns with different cross-sectional aspect ratios. Magazine of Concrete Research, 69(19), 1011–1026. https://doi.org/10.1680/jmacr.17.00036.

Mansour Kadhum Alkafaji, M. (2015). Structural Performance of Short Square Self Compacting Concrete Columns in Fire. Engineering and Technology Journal, 33(1A), 237–256. https://doi.org/10.30684/etj.33.1A.18.

Muthuswamy, K. R., & Thirugnanam, G. S. (2014). Structural behaviour of hybrid fibre reinforced concrete exterior Beam-Column joint subjected to cyclic loading. International Journal of Civil & Structural Engineering, 4(3), 262–273.

Noman, M., Salman, M., Ahmed, A., Hussain, M., Akhtar, A., & Zulqarnain, M. (2025). Repair of Fire-Damaged Circular and Square Columns Using CFRP Composites: A Comprehensive Review. Journal of Civil Engineering Frontiers, 6(02), 82–96. https://doi.org/10.38094/jocef602116.

Noman, M., Yaqub, M., Salman, M., Faizan, M., Mahmoudabadi, S., & Ahmad, A. (2025). Predicting axial load capacity of CFRP fire-damaged RC columns through DANN. Innovative Infrastructure Solutions, 10(12), 571. https://doi.org/10.1007/s41062-025-02371-6.

Salameh, A., Hawileh, R., Safieh, H., Assad, M., & Abdalla, J. (2024). Elevated Temperature Effects on FRP–Concrete Bond Behavior: A Comprehensive Review and Machine Learning-Based Bond Strength Prediction. Infrastructures, 9(10), 183. https://doi.org/10.3390/infrastructures9100183.

Sarsam, K., Khalel, R., & Hadi, M. (2018). Influence of Spirals on the Behavior of Short RC Columns Strengthened by External CFRP. Engineering and Technology Journal, 36(2A), 223–233. https://doi.org/10.30684/etj.36.2A.15.

Shin, J., Lee, H., Choi, I.-R., Min, J.-K., & Choi, S.-M. (2024). Fire performance of CFRP-strengthened piloti-type columns with fire-resistant materials during standard fire exposure. Scientific Reports, 14(1), 23597. https://doi.org/10.1038/s41598-024-74306-7.

Yoo, S.-W., & Choo, J. F. (2022). Behavior of CFRP-reinforced concrete columns at elevated temperatures. Construction and Building Materials, 358, 129425. https://doi.org/https://doi.org/10.1016/j.conbuildmat.2022.129425.

Zhao, J., Wang, S., Wang, Z., Wang, K., & Fu, C. (2023). Bond performance between FRP bars and geopolymer concrete after elevated temperature exposure. Construction and Building Materials, 384, 131476. https://doi.org/https://doi.org/10.1016/j.conbuildmat.2023.131476.

Zhou, J., Zhou, Y., Guo, M., & Xiang, S. (2026). Fire Performance of FRP-Composites and Strengthened Concrete Structures: A State-of-the-Art Review. Polymers, 18(2), 181. https://doi.org/10.3390/polym18020181.

How to Cite This Article

Mousa, M. W., Mohammed, A. S., & Abdulqader, S. S. (2026). Post-Fire Performance Enhancement of Pre-loaded RC Short Columns Using CFRP Confinement. Civil and Environmental Engineering, 0 (0). https://doi.org/10.2478/cee-2026-0109